

Elastic waves in the presence of a granular shear band formed by direct shearQi Zhang,¹ Yinchang Li,¹ Meiying Hou,¹ Yimin Jiang,² and Mario Liu³¹*Beijing National Laboratory for Condensed Matter Physics, Institute of Physics, Chinese Academy of Sciences, Beijing 100190, China*²*Central South University, Changsha 410083, China*³*Theoretische Physik, Universität Tübingen, D-72076 Tübingen, Germany*

(Received 14 December 2011; published 22 March 2012)

The propagation of elastic waves in a box under direct shear, filled with glass beads and being sheared at constant rates, is studied experimentally and theoretically. The respective velocities are shown to be essentially unchanged from that in a static granular system under the same pressure and shear stress but without a shear band. Influence of shear band on sound behaviors are also briefly discussed.

DOI: [10.1103/PhysRevE.85.031306](https://doi.org/10.1103/PhysRevE.85.031306)

PACS number(s): 45.70.Cc, 43.25.+y, 83.60.Uv

I. INTRODUCTION

Granular media are known to display both elastic and plastic behavior [1]. A pronounced elastic behavior is the propagation of longitudinal and transverse waves, quite similar to that in an elastic system [2] (see also Ref. [3] for the study of nonlinear effects at higher amplitudes). On the other hand, the critical state of granular media displays striking plastic behavior [4]: When being sheared at a constant rate, the shear stress of a granular system will, after first increasing as in any elastic system, saturate at a constant value that is independent of the rate. The asymptotic state, ideally plastic, is usually referred to as *critical*. If the initial density is low, the shear stress increases monotonically as the strain accumulates, until it reaches the saturated, critical stress σ_c . If the initial density is high, the shear stress will first go through a maximum σ_M , before arriving at the same σ_c . Frequently, a shear band is formed right after σ_M . Conceptually, it is simply the concentration of shear rate and plasticity within a narrow region. The question we pose here is: How do the elastic and plastic behavior affect each other? More specifically, how is the propagation of elastic waves influenced by the constant shear rate that occurs in a shear band?

Two seemingly straight answers contradict each other when considering the difference between sound propagation in a static granular medium and one that is being sheared: (1) Microscopically, it appears obvious that enduring contacts in a static medium are essential for the transmission of sound. If the system is being sheared slowly enough, such that the contacts remain for a number of wave oscillations, nothing much should change: With d the diameter of the grain, $\dot{\gamma}$ the shear rate, ω the angular frequency of sound wave, $\dot{\gamma}d$ is the velocity difference, which, during the time span of $1/\omega$, should yield a displacement much smaller than d , or $\omega/\dot{\gamma} \gg 1$. (2) Macroscopically, we know that the propagation of waves depends critically on the system being elastic. For an ideally plastic state, stress does not increase for increasing strain, and it has no restoring force. So we must conclude that elastic waves do not exist.

As we shall see, neither answer is quite right. Microscopically, before particles lose contacts due to shearing, something else occurs that kills the waves: The slight jiggling and slipping of the grains produced by the shear rate—quantified by the granular temperature T_g —softens the contacts, relaxes the stress, and restricts wave propagation. Since the jiggling

grows with the shear rate, $T_g \sim \dot{\gamma}$, so does the restriction. As shown below, the existence of elastic waves depends on the inequality, $\omega/\dot{\gamma} \gg \Lambda$, where typically $\Lambda \approx 10^2$ for sand. So this condition is rather more stringent than $\omega/\dot{\gamma} \gg 1$. Macroscopically, the critical state may be seen as a stationary solution, in which the rate of stress increase produced by a given shear rate is just the amount being relaxed [5]. Therefore, additional stress fluctuations given by an elastic wave no longer relax, and (if varying fast enough) will propagate as a wave signal. (In contrast to the work in Ref. [6], we consider only normal incidence of the sound. Also, sound amplification due the presence of a shear band as considered in Ref. [7] is ignored.)

We employ granular solid hydrodynamics (GSH) [8] to evaluate wave propagation, starting from an appropriate elastic energy and assuming that the anisotropy is predominantly stress-induced. As shown in Ref. [9], the propagating velocities of elastic waves as a function of the applied external stress are well accounted for. When the medium is being sheared, two additional effects need to be included: The associated slipping and jiggling of the grains and the softening of the granular contacts.

The macroscopic stress is maintained by the elastic deformation of the grains. When the grains slip and jiggle, they briefly lose contact with one another, during which some of their elastic deformation is lost, and the macroscopic stress relaxes, leading to an enhanced damping mechanism characteristic of the granular system. For $\omega/\dot{\gamma} \lesssim \Lambda$ (i.e., when the effect is too strong), the collective modes of elastic waves become diffusive and no longer propagate. Mathematically speaking, this is analogous to propagation of electromagnetic waves in conductors.

When granular contacts soften, and the effective elastic stiffness decreases by the factor $(1 - \alpha)^2$ in GSH (with α of the order of 0.8; see Ref. [10]), the wave velocity $\sim 1 - \alpha$ is reduced by a factor of five. Microscopically, this may be related to force chains being disrupted by shear rates, as the system is softer when less force chains are present. (A minimal number of force chains remain robust, as these are needed to maintain the system's mechanical stability.) Mathematically, this is analogous to a dielectric permeability of $(1 - \alpha)^{-2}$.

In a system containing a shear band, an elastic wave propagates in the static solid region and traverses the shear band. The propagation in the static region remains unchanged

from that in a static system without a shear band. In the shear band—assuming it is in the continually deforming, stationary critical state—elastic waves will propagate but are subject to the above two effects. The behavior is similar to an electromagnetic wave propagating in vacuum and traversing a conducting layer with a large dielectric permeability. In a time-of-flight experiment, if the shear band is narrow, the wave is in the solid region most of the time. Therefore, the averaged velocity should not change much by the presence of the shear band. Neither should the amplitude change much due to the enhanced damping mechanism. So generally speaking, propagation of elastic waves is not a sensitive probe for the presence of shear bands. On the other hand, the significantly reduced wave velocity in the shear band implies that there will be considerable reflection at the rim of the shear band, or the elastic-plastic boundary, which should further reduce the magnitude. Unfortunately, this is not easily observed: Due to considerable multiple scattering in granular media, the wave velocity is usually measured at the leading edge, while the coda wave, containing almost all of the wave energy, is neglected [2]. Observing a further reduction of the already strongly diminished leading edge requires cleaner experiments than is usually given.

Previously, Khidas and Jia have performed similar experiments [11] in the same setup. The differences are twofold: First, the two-leg shear they applied is avoided here, which eliminates a source of uncertainty; second, though the experimental data are comparable, they seem to have concluded that the presence of shear band is felt by the velocity of the elastic wave, which is in contradiction to our main conclusion.

The experiments and simulation of Hostler and Brennen [12] concentrate on sound in granular media, but they probed the depth of its complexity by varying a number of conditions, including: grain size and form, glass and PVC, the duration of pulse, frequency, and transducer geometry. Most notably, they observed sound propagation while the granular bed is being shaken. When aiming to interpret their results using GSH, one needs to be aware that although GSH includes all dissipative mechanisms, especially plastic deformations such as rearrangements of grains and force chains, it is a macroscopic theory that holds only in the robust and universal limit of long wave lengths, in which individual force chains, however fragile and ephemeral, are averaged over. This is the same limit of coherent wave propagation in different force chains that Jia *et al.* studied [2]. Most of the data in Ref. [12] are not in this limit. Moreover, although GSH gives the sound velocity as a function of T_g and the static stress, shaking the granular bed (the upper side of which is open) changes T_g and the static stress at the same time, without any separability. This renders a comparison to GSH's results difficult. Also, the finding that pressure change is detected at the second transducer up to a shaking acceleration of $2g$ unfortunately does not discriminate whether the pressure pulse is being propagated or diffused—the two limits of our theory; see Sec. III B—again making a comparison difficult.

II. EXPERIMENT

A schematic diagram of the experimental setup is shown in Fig. 1. Our samples consist of randomly packed glass beads

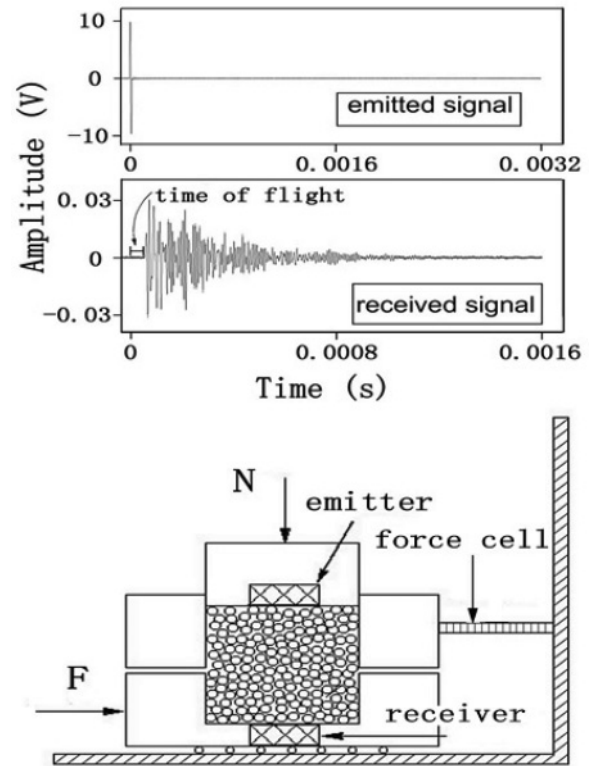


FIG. 1. Experimental setup, with a typical emitted and received signal.

of diameter $d = 1.7\text{--}2.0$ mm in a direct shear apparatus, $S = 70 \times 70$ mm. The total inner height of the cell is 49 mm, separated into two parts with the top part of 26 mm and the lower one of 23 mm. The total mass of the glass beads is $M = 355 \pm 0.5$ g. Samples are prepared by tapping the sidewall of the box to reach a compact packing of the volume fraction 0.648 ± 0.002 . The density of glass bead is 2441 kg/m^3 . A normal load N , corresponding to the apparent pressure in the range of 183–366 kPa is applied to the top cell. At such a load level, the influence of gravity can be neglected.

The lower cell sitting on a steel ball bearing is pushed by a motor at a constant speed, $v_0 = 13.3 \mu\text{m/s}$, while the top part is connected to a fixed digital ring force gauge. The stiffness coefficient of the force gauge is $5.25 \times 10^5 \text{ N/m}$. The shear stress is measured by the ring force gauge. Two dial gauges are used to measure the displacements of the upper and lower cells. Figures 2(a) and 2(b) show variations of the shear stress σ_{xz} and averaged density $\rho = M/hS$, where h is the momentary height of the shear box, measured by the top force gauge, with the shear displacement of $x = v_0 t$. The stress variations are similar to illustrations in soil mechanic textbooks. They have a peak value that increases linearly with the top load, after which the stress approaches a stationary value (not fully reached). As all our samples have high initial densities, they dilate with shearing.

A large wave transducer (of diameter 45 mm) is placed at the center of the inner surface of the top cell, and a smaller receiver (of diameter 10 mm) is fixed to the center of the inner surface of the bottom cell. A sinusoidal pulse of frequency $f = 50 \text{ kHz}$, generated every 0.02 second, is emitted from

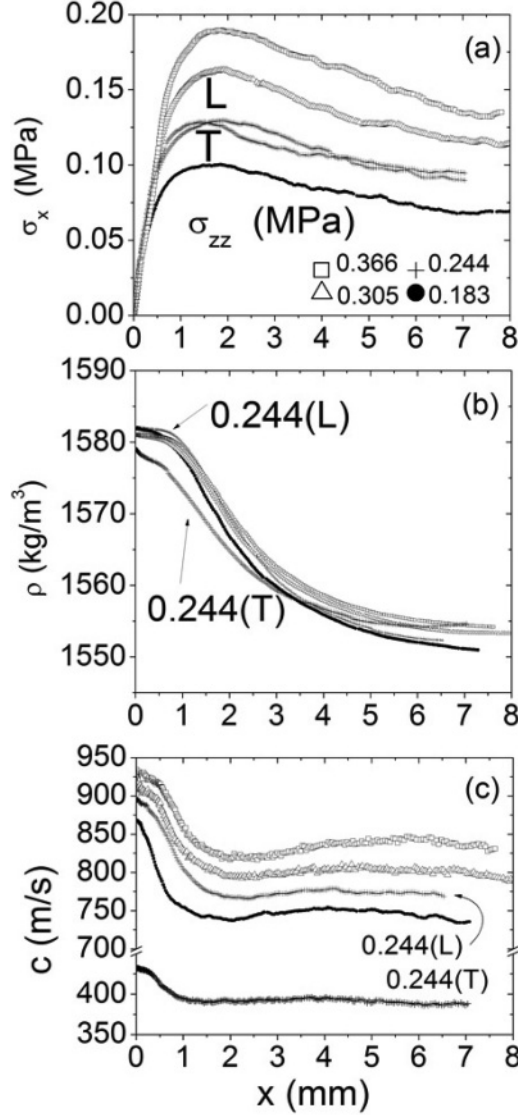


FIG. 2. Evolution of the shear stress (a), the average density (b), and sound velocity (c) for the shear box experiment.

the transducer through the granular bed to the receiver. The emitted and received signals such as rendered in Fig. 1, are recorded by an oscilloscope. In our experiment, the wavelength is approximately $2 \text{ cm} \gg d$. Since it is much larger than the particle diameter, the scattered waves are quickly attenuated. We measure the time-of-flight of the coherent wave t_f and divide it by the traveled distance L , the thickness of the granular bed, obtaining velocity $c = L/t_f$.

The longitudinal sound velocity is measured for four different top loads, $N = 0.183, 0.244, 0.305$, and 0.366 MPa, while the transverse velocity is measured only for one top load, 0.244 MPa. Initial densities of the samples vary slightly from 1579 to 1582 kg/m^3 . The experimental results are shown by symbols in Fig. 2(c). The measured velocities decrease about 10% as the shear stress σ_{xz} varies from 0 to its maximum σ_M and then increases slightly ($<2\%$). The transverse velocity has a similar behavior but is about half the speed of the longitudinal ones—consistent with the observation in Ref. [11].

III. EVALUATION OF WAVE VELOCITIES

We use a purely elastic approach to calculate the velocity of elastic waves for the solid region. In the present experiment of constant normal pressure and shear rate, the shear stress and density vary with time. As the initial density is consolidated, the stress undergoes a maximum. The wave velocity is evaluated assuming a series of static states with the same pressure, stresses, and density. And the results agree well.

A. In a static granular medium

According to the elasticity theory, for the case of plane waves propagating in a sample of uniform stress, the velocities are given by the square roots of the eigenvalues of the following matrix [13] (summation on repeated foot indices is assumed),

$$S_{ij} = M_{imnj} \hat{k}_m \hat{k}_n / \rho, \quad (1)$$

where ρ is mass density, $\hat{k}_n = k_n / \sqrt{k_i k_i}$ the unit wave vector, and M_{imnj} the stiffness tensor, given as the derivation of the stress σ_{im} with respect to the elastic strain u_{nj} ,

$$M_{imnj} = \partial \sigma_{im} / \partial u_{nj}. \quad (2)$$

Moreover, the stress is given by deriving the elastic energy density $w = w(\rho, u_{ij})$,

$$\sigma_{im} = -\partial w / \partial u_{im}. \quad (3)$$

Using Eqs. (1)–(3), wave velocities can be calculated as functions of density and stress, $c = c(\rho, \sigma_{ij})$, after the $w(\rho, u_{ij})$ is given. For the simplest case, w is a quadratic function of u_{ij} , implying linear elasticity, for which c is independent of the stress σ_{ij} . The elasticity of granular matter is nonlinear, and wave velocities depend on both the density and stress.

A simple yet fairly realistic elastic potential w for cohesiveless granular matter is [8,10]

$$w = B_0 B_\rho \sqrt{\Delta} (\Delta^2 + 3u_s^2/2), \quad (4)$$

where $\Delta \equiv -u_{kk}$ and $u_s \equiv \sqrt{u_{ij}^* u_{ij}^*}$ (with $u_{ij}^* \equiv u_{ij} + \Delta \delta_{ij}/3$) are bulk and shear strain, respectively. B_ρ is a density-dependent factor:

$$B_\rho = \left(\frac{\rho/\rho_c - \rho_1}{1 - \rho/\rho_c} \right)^{0.15}. \quad (5)$$

It accounts (1) for the softening of the granular matter when it becomes looser; and (2) for the fact that the density of granular solids cannot go below the random loose packing density ρ_ℓ and cannot exceed the random close packing density ρ_c . (Note $9\rho_1 = 20\rho_\ell/\rho_c - 11$; see Ref. [8] for details.) We take $\rho_\ell = 0.85\rho_c$, with $\rho_1 = 0.67$, $B_0 = 2.36 \text{ GPa}$, and $\rho_c = 1585 \text{ kg/m}^3$.

When analyzing the wave velocities in a shear box as outlined above, density and stress inhomogeneities in the samples, together with the associated fluctuation of the velocity, are neglected. However, in a time-of-flight experiment, one measures the averaged velocity, which may approximately be taken as a function of the averaged stress and density.

Given the stress and density, the nonlinear elasticity rendered by Eqs. (1)–(5) describes completely the wave velocities. For the shear box we use, only two components of σ_{ij} , the top load $\sigma_{zz} = N$ and the shear force $-\sigma_{xz} = F$ (as shown in

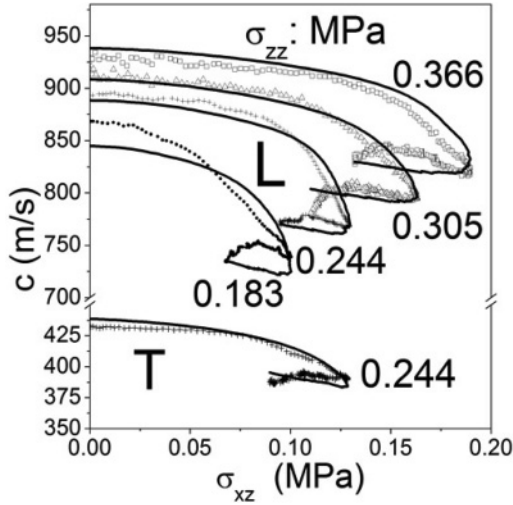


FIG. 3. A failure geometry used for estimation of stresses inside the shear box.

Fig. 3), can be measured. The other components need to be estimated, usually by assuming that the principle axis of the maximum stress has the angle $\theta = 45^\circ + \varphi/2$ with respect to the shear band, where φ is the internal friction angle. (This is a widely adopted assumption in soil mechanics [1].) The other two principle stresses we take to be degenerate. Consequently, our samples are subject to the isotropic stress: $\sigma_{ij} = N\delta_{ij}$ for $F = 0$. These circumstances are shown in Fig. 3, in which x', y', z' denote axes of principle stresses with z' being the maximal one, and x, y, z the coordinates for computing sound velocities. From the principle stresses $\sigma_1 = \sigma_2 = N - F \cot \theta$ and $\sigma_3 = N + F \tan \theta \geq \sigma_1$, we obtain the following stress tensor in x, y, z :

$$\sigma_{ij} = \begin{pmatrix} N + F \left(\frac{\sin^2 \theta}{\cot \theta} - \frac{\cos^2 \theta}{\tan \theta} \right) & 0 & -F \\ 0 & N - \frac{F}{\tan \theta} & 0 \\ -F & 0 & N \end{pmatrix}. \quad (6)$$

For glass beads, we choose a typical value $\varphi \sim 27^\circ$ for the internal friction angle. Using the stress tensor Eq. (6), the wave velocities $c(\rho, N, F)$ are calculated. The results are rendered

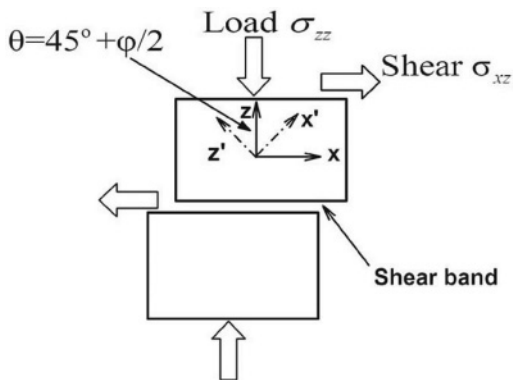


FIG. 4. Variation of wave velocities with shear stress, for the shearing process described in the legend of Fig. 2. Symbols are measurements; full curves are results of GSH.

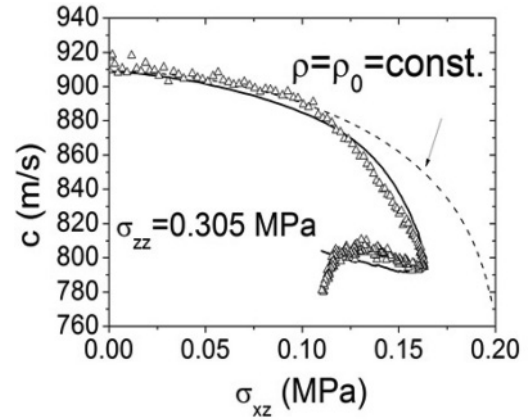


FIG. 5. Dashed curve, sound velocity at constant density. Symbols and full curve are the same as described in the legend of Fig. 4.

as full curves in Fig. 4, as function of the measured ρ, N, F from Fig. 2. The agreement is good.

Figure 5 illustrates the effect of density dependence, which, if taken as constant (the initial density of 1581 kg/m^3 , in addition to $N = 0.305 \text{ MPa}$), would not yield the curves of Fig. 4. Rather, the wave velocity as depicted decreases monotonically with F . The measured curve has a turning point, around which there are two velocities for the same F , though at different densities.

B. Influence of shear band

For a brief estimation of influence of shear band on the above elastic results, we start with two basic equations of GSH:

$$\rho \partial_t v_i - (1 - \alpha) \nabla_m K_{imkl} u_{kl} = 0, \quad (7)$$

$$\partial_t u_{ij}^0 - (1 - \alpha) v_{ij}^0 = -\lambda T_g u_{ij}^0. \quad (8)$$

(For simplicity, we concentrate on shear waves, assuming $v_{\ell\ell} \equiv 0$.) The first equation accounts for the conservation of momentum and the second for the motion of the elastic stress [8]. For $\alpha, T_g = 0$, they reduce to the simple elasticity theory employed in the last subsection.

The granular temperature T_g quantifies the excitation of grains, how they slip and jiggle. For small shear rates $\dot{\gamma}$ (such as accompanying an elastic wave through a static granular medium), we have $T_g \sim |\dot{\gamma}|^2$, and we may neglect the quadratically small relaxation term $-\lambda T_g u_{ij}^0$. For larger $\dot{\gamma}$, we have $T_g \sim |\dot{\gamma}|$, and we may again neglect the variation in $|\dot{\gamma}|$ that accompanies an elastic wave, because the dynamics of T_g is too slow to follow the oscillation of the wave. The off-diagonal Onsager coefficient $\alpha = \alpha(T_g)$ vanishes for $T_g \sim \dot{\gamma}^2 \rightarrow 0$ and quickly saturates at constant shear rates $\dot{\gamma}$ (for both shear rates of the experiment because of the minimal number of force chains mentioned above).

Taking $\alpha \approx 0.8$ and rewriting $\lambda T_g = \lambda \sqrt{\eta/\gamma} |v_{ij}^0| \equiv \Lambda |v_{ij}^0|$, with $\Lambda \approx 10^2$, we combine Eqs. (7) and (8) to obtain the telegraph equation

$$\partial_t^2 \bar{u} = (c^2 \nabla_x - \Lambda \dot{\gamma} \partial_t) \bar{u}, \quad (9)$$

for the amplitude $\bar{u} \sim e^{iqx-i\omega t}$, of an eigenvector for the elastic wave, propagating along \hat{x} , where the new wave velocity c , denoted as

$$c = (1 - \alpha)c_{\text{static}}, \quad (10)$$

is reduced by the above factor from its static value c_{static}^2 , given by the eigenvalues of Eq. (1) [14].

Inserting $\bar{u} \sim e^{iqx-i\omega t}$ into Eq. (9), we find

$$c^2 q^2 = \omega^2 + i\omega\Lambda\dot{\gamma}, \quad (11)$$

implying, for the high-frequency limit $\omega \gg \Lambda\dot{\gamma}$,

$$q \approx \pm \frac{\omega}{c} \left(1 + i \frac{\Lambda\dot{\gamma}}{2\omega} \right) = \pm \left(\frac{\omega}{c} + i \frac{\Lambda\dot{\gamma}}{2c} \right), \quad (12)$$

and simple diffusion for the low frequency limit, $\omega \ll \Lambda\dot{\gamma}$,

$$q \approx \pm \frac{\sqrt{\omega\Lambda\dot{\gamma}}}{c} \frac{1+i}{\sqrt{2}}. \quad (13)$$

With the shear rate of the experiment $\dot{\gamma} \lesssim 1/s$, and the frequency of the elastic wave $\omega \gtrsim 10^3/s$, the condition of the high-frequency limit $\omega \gg \Lambda\dot{\gamma}$ is satisfied. Inserting Eq. (12) into $\bar{u} \sim e^{iqx-i\omega t}$, the wave form is

$$\exp \left[-i\omega \left(t \mp \frac{x}{c} \right) \mp x \frac{\Lambda\dot{\gamma}}{2c} \right]. \quad (14)$$

The first term accounts for wave propagation, the second a frequency-independent decay length $2c/\Lambda\dot{\gamma}$. In contrast, the reduction of c is rate-independent. It is worth it to note that the reduction is not observed by the present time-of-flight experiment because the shear band is too thin in comparison with the height of shear box. The decay in the Eq. (14) may

exist in The received signal, but we cannot separate it out because it is too complicated by multiple scattering.

IV. DISCUSSION AND CONCLUSION

The propagation of elastic wave depends on the stress, density, and the level of granular jiggling quantified as T_g . Our measurements of wave velocities employing the time-of-flight method are capable of showing the first two dependencies but proves less appropriate for probing the influence of T_g , which according to GSH changes both the velocity and the damping. Since T_g is present only inside the shear band, which is rather narrow, we may neglect its influence on the velocity in a time-of-flight experiment. The comparison of theory and experiment presented above shows the validity and accuracy of the present setup for determining the elastic potential and its parameters employed in GSH.

The influence of T_g on damping is measurable, and with it also the influence on the received total signal strength. We observe a change of the signal due to the presence of the shear band, where especially the amplitude of the signal's first cycle decreases by a factor of three. Although the received signal is dispersed and complicated (see the inset of Fig. 1), with the first cycle being a very small portion of the total signal, this behavior seems suggestive of the reflection discussed in the last section. However, before any conclusions may be drawn, we need to return, in a future paper, to undertake a more detailed study.

ACKNOWLEDGMENTS

This work is supported by the National Natural Science Foundation of China (Grant No. 11034010) and special fund for earthquake research (Grant No. 201208011).

-
- [1] G. Gudehus, *Physical Soil Mechanics* (Springer-Verlag, Berlin, 2011); G. Gudehus, Y. M. Jiang, and M. Liu, *Granular Matter* **13-4**, 319 (2011).
- [2] X. Jia, C. Caroli, and B. Velicky, *Phys. Rev. Lett.* **82**, 1863 (1999); X. Jia, *ibid.* **93**, 154303 (2004).
- [3] V. Tournat and V. E. Gusev, *Phys. Rev. E* **80**, 011306 (2009); C. Inerra, V. Tournat, and V. E. Gusev, *Appl. Phys. Lett.* **92**, 191916 (2008).
- [4] A. Schofield and P. Wroth, *Critical State Soil Mechanics* (McGraw-Hill, London, 1968); D. M. Wood, *Soil Behavior and Critical State Soil Mechanics* (Cambridge University Press, Cambridge, 1990).
- [5] S. Mahle, Y. M. Jiang, and M. Liu, e-print [arXiv:1006.5131v3](https://arxiv.org/abs/1006.5131v3).
- [6] C. Caroli and B. Velicky, *Phys. Rev. E* **67**, 061301 (2003).
- [7] L. Bonneau, T. Catelin-Jullien, and B. Andreotti, *Phys. Rev. E* **82**, 011309 (2010).
- [8] Y. M. Jiang and M. Liu, *Granular Matter* **11**, 139 (2009).
- [9] M. Mayer and M. Liu, *Phys. Rev. E* **82**, 042301 (2010).
- [10] Y. M. Jiang and M. Liu, *Phys. Rev. Lett.* **91**, 144301 (2003); **99**, 105501 (2007).
- [11] Y. Khidas and X. Jia, in *Powders and Grains 2009*, edited by M. Nakagawa and S. Luding (2009), pp. 259–262.
- [12] S. R. Hostler and C. E. Brennen, *Phys. Rev. E* **72**, 031303 (2005).
- [13] L. D. Landau and E. M. Lifshitz, *Theory of Elasticity*, 3rd ed. (Pergamon Press, New York, 1986).
- [14] The density in the shear band is generally lower than in the solid. This will further reduce c^2 .